Research on Engineering Structures & Materials
www.jresm.org
Research Group

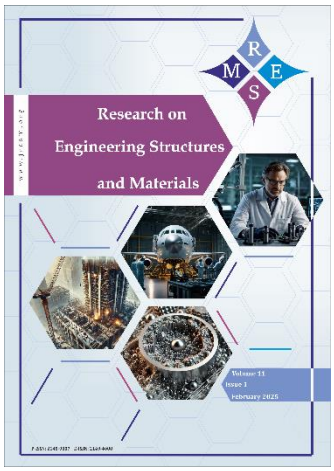

Prototype silicone rubber based passive seismic damper: Development, characterization and implementation

Utsav Koshtia, Sharadkumar Purohit

Online Publication Date: 20 May 2024
URL: http://www.jresm.org/archive/resm2024.201ma0229rs.html
DOI: http://dx.doi.org/10.17515/resm2024.201ma0229rs

Journal Abbreviation: *Res. Eng. Struct. Mater.*

To cite this article
Koshtia U, Purohit S. Prototype silicone rubber based passive seismic damper: Development, characterization and implementation. *Res. Eng. Struct. Mater.*, 2025; 11(1): 139-163.

Research on Engineering Structures & Materials
www.jresm.org
Research Group

Research Article

Prototype silicone rubber based passive seismic damper: Development, characterization and implementation

Utsav Koshti[a], Sharadkumar Purohit[*,b]

Dept. of Civil Eng., School of Engineering, Institute of Technology, Nirma University, Ahmedabad, India

Article Info

Article history:

Received 29 Feb 2024
Accepted 14 May 2024

Keywords:

Silicone rubber;
Kelvin-Voigt model;
Benchmark building;
Passive damper

Abstract

Passive damping devices are mostly preferred owing to their relatively lower cost, low maintenance, and stability over a wide range of frequencies during seismic events. Currently, these devices with temperature in-sensitive viscoelastic material are being explored. The paper aims to develop a prototype piston-cylinder based passive damper with silicone rubber particles and characterize it with varied amplitude and frequency of sinusoidal input. The device Silicone Rubber Particle Packed Damper, so developed, was then implemented in the benchmark building for seismic response control. Silicone rubber particles with lower hardness were produced through compressed molding technology to improve the damping efficiency of the device. The device was later converted to an Air Damping Device by removing silicone rubber particles for a natural comparison of efficacy. Hysteresis curves of devices, elliptical in shape, obtained through characterization were mathematically modelled using the Kelvin-Voigt model, and parameters were identified using multivariable linear regression to implement them with the benchmark building. Uncontrolled and controlled responses of benchmark building fitted with, both, damping devices were determined under strong motion (El Centro, Hachinohe) and pulse-type (Kobe, Northridge) seismic excitations. Seismic response parameters; peak displacement, peak interstorey drift, peak acceleration, and peak damper force was estimated. Each seismic response parameter yields substantial reduction for controlled benchmark building with Silicone Rubber Particle Packed Damper. The efficacy of damping devices was established by Performance Indices in terms of peak interstorey ratio, level acceleration, base shear, and control force. Though both passive damping devices were found effective in seismic response control of benchmark building, Silicone Rubber Particle Packed Damper outperforms Air Damping Device. The developed prototype damping devices are a low cost and easy to maintain.

1. Introduction

Earthquakes, one of the natural disasters, are the most destructive force in nature as they disrupt infrastructure and human lives. In the last couple of decades, earthquakes contributed nearly about 8,10,000 fatalities, worldwide [1]. The recent past has seen a surge in the frequency of earthquakes, especially in seismically active areas, e.g., Japan (2024), Afghanistan (2023), Turkey (2023), and Italy (2016/17). Such earthquakes cause varied degrees of damage to buildings, public infrastructures, industrial and lifeline structures made from concrete, steel and precast materials that can be identified through field observations [2] and quantified by advanced imagery based techniques [3]. It becomes imperative to enhance the seismic resistance of buildings and structures by employing evolving structural control technologies and reducing seismic vulnerability.

[*]Corresponding author: sharad.purohit@nirmauni.ac.in
[a]orcid.org/0000-0001-8652-5868; [b]orcid.org/0000-0002-2678-4320
DOI: http://dx.doi.org/10.17515/resm2024.201ma0229rs

Retrofitting strategies to improve the reduced stiffness of structural elements through jacketing, fibre wrapping, the addition of lateral load resisting elements and providing passive/active damper are other ways to safeguard buildings and structures from future Earthquakes [4]. Developed countries like the USA, Japan, Italy and New Zealand have proactive retrofitting strategies leading to improved seismic resistance for buildings, as evident in recent earthquakes [5]. In developing countries like India, many buildings are seismically vulnerable and at risk of strong earthquakes with the rapid increase in new construction projects [6].

The earthquake induced structural vibrations can be controlled by modifying mass, stiffness, damping or shape and by externally supplying passive or active counter forces. Various methods of structural control have been implemented successfully, and efforts are going on to improve the efficiency of such methods utilizing the mechanical properties of diversified materials. These advanced structural control methodologies are broadly classified as Active, Passive, Hybrid and Semi-active control. Realizing improved structural seismic response of buildings with the implementation of these control devices, it is recommended that such devices are further improved on energy efficient approaches and reduced cost [7]. Owing to mechanical simplicity, reduced power requirement, and relatively higher controllable force capacity, a semi-active system forms an attractive alternative to an active control system [8]. Numerous studies conducted have proved that such systems, when implemented appropriately, perform better than passive devices and yield at par with the performance of fully active systems. However, acceptance of such a system depends on important parameters like construction cost, long-term effect and maintenance along with improved performance. Additionally, structural systems are a combination of various structural elements and thus, integration of such innovative devices with structural systems becomes complex and challenging. In light of these, research efforts are still continued in developing new and modifying existing passive devices for improved seismic response of structures as they are relatively low-cost, offer less maintenance and ensure safety under seismic events owing to their robustness [9].

Passive energy dissipation devices have been under development for many years, beginning with the 1990's. The fundamental principle of these devices is to decrease the inelastic energy dissipation demand of the framing system of structures [10]. The most common passive devices used for seismic response control are viscous fluid dampers, friction dampers and metallic yield dampers, which are classified as rate-dependent and rate-independent devices. Since viscous damping offered by viscous damper is temperature sensitive and material proportion of friction damper tends to decrease and suffered to fatigue effect, there is a need to develop an innovative passive damper for seismic response control of the buildings. Out of these, rate-depended passive energy dissipation devices are in continuous mode of redevelopment with a major focus on the viscoelastic damper (VED). VED has mechanical properties sensitive to various parameters, such as temperature, strain amplitude, excitation frequency, amplitude, hardness, etc., and thus offers diversified damper configuration compared to other passive energy dissipating devices. The performance of VED is largely dependent on vulcanized viscoelastic materials (VEM) made from a composite material, including matrix, vulcanized system, filler system and anti-ageing system. VEM is required to satisfy specific requirements: (i) damping and loss factor, (ii) reduced heat generation with good heat dissipation, (iii) good working performance, (iv) large temperature range, and (v) good durability properties which are difficult to mate with. Current research work focuses on utilizing innovative VEMs which are less sensitive to temperature variation. Therefore, silicone rubber and Nitrile Butadiene Rubber (NBR) were developed and are being studied as potential alternatives to standard VEMs of VEDs [11]. It has been proposed through experiments that the Kelvin-Voigt model of viscoelasticity within certain conditions can

fairly depict the hysteresis behaviour of VEDs [10]. The model comprises of displacement and velocity components represented by a linear spring placed in parallel to a linear viscous dashpot, respectively, as shown in Figure 1(b) [10].

Recently, Particle Impact Damper (PID) that use silicone rubber, Nitrile Butadiene Rubber etc., are gaining momentum that demonstrate enhanced stiffness and natural damping properties [12]. Owing to particle-particle, particle-wall friction and inelastic collision, the kinetic energy of the particle is dissipated, and thus, the vibration of vibration systems gets attenuated by particle damping devices [13], [14]. Out of various types of configurations of particle damper, piston-based particle damper converts mechanical energy of vibration to elastic energy as piston collide and press particles together. Piston-based particle dampers with and without glass and steel particles were tested under transient vibration by Bai et al. [15] revealed that energy dissipation was due to friction contact of particles while young's modulus has little effect on damping. However, density has a greater effect on overall damping performance.

A novel means of vibration attenuation using Vacuum Packed Particles (VPP) as energy dissipating material was proposed by Bartkowski et al. [14]. Three types of granular ball shaped grains of 3 mm diameters made up of polyethylene were tested under triangular constant loading function. A modified Bouc-Wen hysteresis model was fitted through parameter identification with experimental data that showed good agreement [14]. Toyouchi et al. [16] developed dual-chamber single rod type damper with elastomer particles to improve damping characteristics and damper force. A set of experiments were conducted on the damper with elastomer particles varying in diameters 3, 4 and 5 mm. Parametric studies were carried out in terms of Particle Packing Ratio (PPR), vibration frequency and material of particles of the damper, revealing that damping energy increases in the damper [16].

It has been realized that particle dampers utilizing silicone rubber particles need to be studied beyond their experimental characterization as a potential seismic response control damping device, which has not yet been explored. The reported research studies used a few specific PPRs of the silicone rubber particle and hardness value. An independent experimental investigation on particle damper by fitting the PPR value to the existing study set will expand the data set of similar studies. Further, the use of a lower hardness value for silicone rubber particles than in previous studies may further improve the damping characteristics of particle dampers. The present paper aims to develop a prototype passive energy-damping device filled with silicone rubber particles of hardness value 23 and PPR 0.67. The proposed damper was characterized to understand its hysteresis behaviour under cyclic excitations of varied frequencies and amplitudes. For an immediate comparison of the efficiency of the prototype Silicone Rubber Particle Packed Damper (SPPD), silicone rubber particles were removed from the cylinder converting the device to Air Damping Device (ADD). Later on, the efficacy of developed dampers in seismic response attenuation was studied by fitting the damper devices with three storey Benchmark building [17] at the ground storey only. The hysteresis behaviour of the dampers was studied. It was fitted well with the Kelvin-Voigt model, where two modal parameters, stiffness and damping co-efficient, were identified using the multivariable linear regression method. Seismic response parameters, peak displacement, acceleration, interstorey drift and damper force were evaluated. Performance Indices (PIs) related to interstorey drift ratio, level acceleration, base shear and control force were determined for strong and pulse-type seismic excitations.

2. Development of Prototype Silicone Rubber Particle Packed Damper

This section provides details of a prototype passive damping device developed for seismic response control application during the present study. It covers various parameters and aspects of design considered for the development of the device in the following two Subsections: Piston-based cylinder and elastomer damping material.

2.1. Piston-based Cylinder

A piston-based cylinder, typically employed in a variety of mechanical systems, was repurposed in the present study, firstly filled with ball shaped silicone rubber particles and secondly, without particles but filled with air to be used as seismic response control devices. It comprises a cylinder of 50 mm diameter and 2.7 mm thickness supported by a square accumulator of 63 mm × 63 mm dimensions with an air valve of diameter 8 mm at both ends of the cylinder. The cylinder with the accumulator is a single casting aluminum body with a screwing mechanism so the accumulator can be detached from the cylinder part. A piston has a 305 mm rod connected with a circular plate of 35 mm thickness and 20 mm diameter at one end and is made of stainless steel. Overall assembly of the cylinder with an end framing system are made airtight.

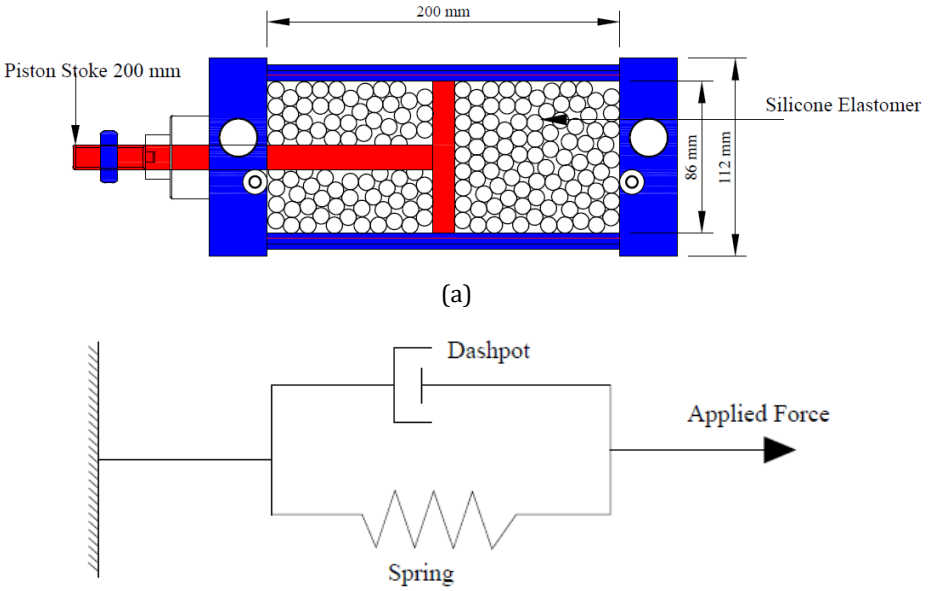

Fig. 1. Pistone based cylinder damper (a) schematic diagram (b) Kelvin-Voigt mathematical Model [10]

Thus, air can only travel in and out of the cylinder through the air valve provided at each end, which acts upon the pressure-suction principle. The piston-based cylinder packed with silicone rubber particles with the central position of the piston is shown schematically in Figure 1(a). The mathematical model of the damper described in section 5 is shown in Figure 1(b). The device has a maximum peak-to-peak displacement amplitude of ±20 mm and is lightweight, having 2 kg weight with air and 2.2 kg weight with silicone rubber filled inside the cylinder. The device was developed with the aim of implementing it with the benchmark building problem [17] with negligible mass vis-à-vis storey mass. The device provides flexibility to carry out damping characteristic studies using a variety of

elastomers, nitrile butadiene rubber (NBR) and other materials under cyclic excitation in the laboratory, repetitively establishing the robustness of the piston-based cylinder device. The fabrication cost of a piston-based device is approximately INR 4725, and the same can be procured commercially at a reasonable price with respect to its fabrication cost. The device doesn't require any additional accessories and preparation before using as a passive damping device for cyclic testing.

2.2 Elastomer Damping Material

Rubber, a class of viscoelastic materials, is a composite material comprising of matrix, vulcanization system and anti-ageing system. There are two types of matrices, currently widely used, natural rubber and synthetic rubber. As compared to natural rubber, synthetic rubber can be more effectively produced with controllable chemical and physical properties. The Vulcanization process includes melting of rubber in the mold with high pressure to convert elastomer into elastic and dimensionally stable form and to yield temperature independent physical properties. Figure 2 shows silicone rubber produced through a compressed molding process in a ball shape with 5 mm diameter by heating followed by cooling to form the shape. At a time, 56 nos. of silicone rubber particles can be produced with the mold fabricated from stainless steel material. It also shows silicone rubber particles are consistent in dimension, weight and homogeneity. The weight of single silicone rubber particles was evaluated and reported in Table 1. The particle packing ratio, also referred as packing fraction [15] is defined as,

$$PPR = \frac{Total\ mass\ of\ the\ Particles}{Volume\ of\ the\ space\ in\ the\ container \times Density\ of\ the\ Particle} \quad (1)$$

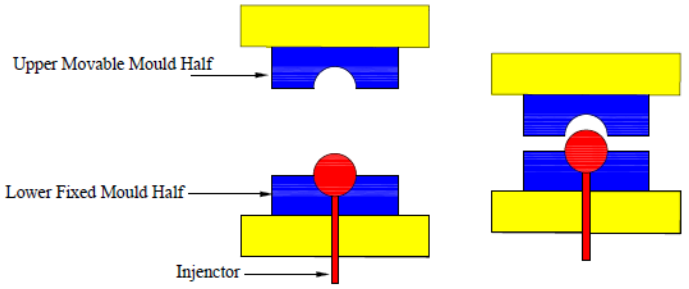

(a)

(b)

Fig. 2. Compression molding process of silicone rubber particle production and silicone rubber particles

The PPR evaluated using Equation (1) was 0.65, which is different than the PPR considered in other research [14], [15] and, thus, adds value to the existing set of research outcomes. Additionally, these research studies have used elastomer particle damping material with durometer hardness values ~ 60, classified as harder than the hardness value of 23, indicating soft material for shore A scale of durometer, measured for the produced silicone rubber particle for the study. This will improve the damping characteristic of silicone rubber particles as soft particles will undergo relatively larger deformation under sinusoidal input to the damping device. The silicone rubber particle with lower density, when used to fill space in a piston-based cylinder shall not greatly increase the mass of the SPPD.

Table 1. Physical and mechanical properties of silicone rubber particle

Material Type	Identification No.	Diameter (mm)	Density (g/cm^3)	Particle Packing Ratio	Durometer Hardness (Shore A)	Tensile Strength (MPa)
Silicone Elastomer	KE-520 -U	5	1.06	0.67	23	11

3. Characterization of Silicone Rubber Particle Packed Damper:

A detailed experimental program was developed to characterize SPPD in terms of hysteresis behaviour under varying frequencies and amplitude of the sinusoidal dynamic input. Characterization studies were conducted in two phases: firstly, SPPD, with a Particle Packing Ratio of 0.65, was tested and secondly, silicone particles were removed from the piston-based cylinder and the volume of the space in the cylinder was left with the atmospheric air transforming SPPD to ADD. A specialized experimental test set-up comprising a dynamic loading frame with a hydraulic piston controlled by an electric stepper motor capable of varying frequency was prepared at the workshop laboratory by the mechanical engineering department. The loading frame is capable of imposing cyclic loading to the attached specimen in the forcing frequency ranges between 0.5 Hz to 3.5 Hz through adjustable variable drive depending upon amplitude ranges from 5 mm to 40 mm. A specialized attachment was fabricated to connect the piston of SPPD with the hydraulic piston of the dynamic loading frame. An instrumental layout for the measurement of force and displacement was prepared. A dynamic force transducer of capacity 500 kg was installed between the reaction beam of the frame and the bottom of the piston-based cylinder having piston attachment assemblies. A piezoelectric based accelerometer of 10 g capacity was attached with a reciprocating plate connected to the hydraulic piston of the frame. Both force and acceleration sensors were attached to the data acquisition system-National Instruments (NI) for logging real-time force and acceleration data. The data acquisition system was connected to the computer system for compilation and post-processing of the data. Acceleration measurement in real-time was integrated twice to measure displacement input to the SPPD. A bandpass filter was used to remove noises from the measurement. A schematic diagram of the experimental set-up comprising of dynamic loading frame SPPD device, damper, force and acceleration sensors, data acquisition system and computer system is shown in Figure 3.

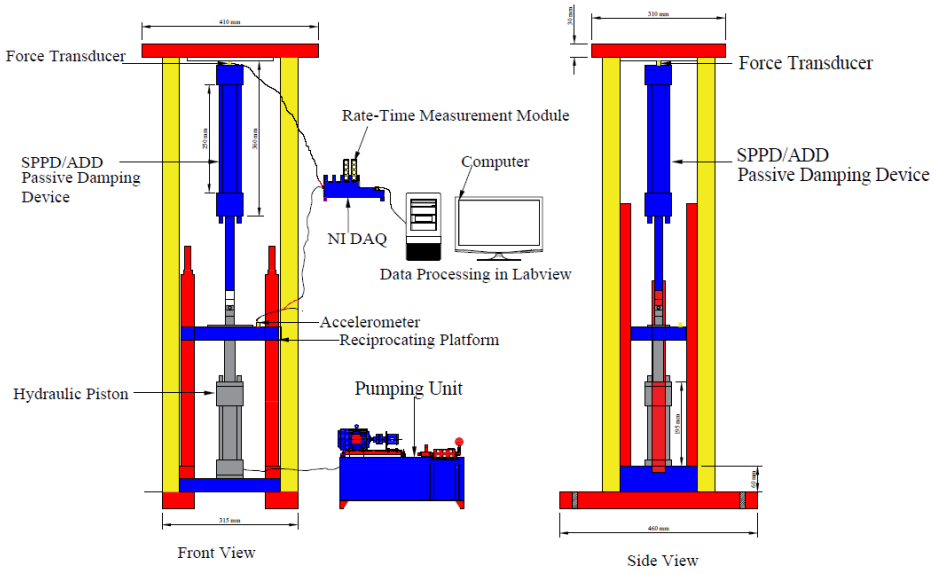

Fig. 3. Schematic diagram of experimental test set-up and instrumentation diagram for characterization of SPPD and ADD

Three sets of displacement inputs were applied to the SPPD and ADD through the hydraulic piston of the dynamic loading frame, as shown in Table 2.

Table 2. Details of sinusoidal displacement input used for characterization of passive damping devices

Displacement Input	Amplitude (mm)	Forcing Frequency (Hz)
Sinusoidal	~ 5	0.5, 1, 2, 3, 3.5
	~ 10	0.5, 1, 1.5, 2
	~15	0.5, 1

It is evident from Table 2 that as the amplitude of displacement input increases, the forcing frequency applied decreases, and thus experiments related to few frequencies for 10 mm and 20 mm amplitude could not be performed. It should be observed that the amplitude of displacement is controlled by a proxy sensor attached to the main columns of the loading frame. There are two proxy sensors for controlling peak-to-peak displacement amplitude with an adjustable knob to set the required displacement amplitude input. It was realized that achieving consistent displacement amplitude with different frequencies offers challenges as the proxy sensor controls peak amplitude when reciprocating the platform sensed by it while passing across it over its circular surface on covering some part of it to reverse the velocity of the platform. It was observed that with increasing frequency of the input displacement, the peak displacement amplitude set to a particular number was overshooted. Thus, despite center-to-center displacement between two proxy sensors, fixed displacement amplitude shows variation either higher or lower for different frequency inputs.

The prototype SPPD device was developed with the objective to implement it for seismic response control of building structures. Therefore, it was decided to study the prototype SPPD under earthquake predominant ground motions comprising of strong motion and pulse-type seismic excitation to assess the efficacy of damping characteristics of the SPPD.

Two strong ground motions, El Centro and Hachinohe excitation and two pulse-type ground motions, Kobe and Northridge ground motions, were selected from the seismic excitations data set and the frequency content of each seismic excitation was evaluated through Fast Fourier Transform (FFT) analysis. Table 3 reports peak amplitude, acceleration, velocity and displacement along with predominant frequencies of the seismic excitations. It is evident that predominant frequencies across all seismic excitation ranges between 0.5 Hz to 7 Hz. Therefore, forcing frequencies of sinusoidal displacement inputs were applied between 0.5 Hz to 3.5 Hz, where the upper value of forcing frequency was driven by the maximum amplitude of displacement that aimed to be applied by the dynamic loading frame. Since the characterization of SPPD and ADD should be carried out under varying frequencies and amplitudes of the input sinusoidal displacement loading, various levels of frequencies and amplitude were considered for the present study, as defined by Table 3. In the very recent past piston-type cylinder dampers with viscoelastic material were developed, tested and implemented for vibration response control [14], [16]. However, most of these dampers were found to exhibit no/weak damper force while piston is pulled from its mean position. Additionally, most of these damping devices were used for mechanical and aerospace systems and implementation of such devices for seismic response control of building structures is yet to be explored. The present study, thus, focuses on developing low cost, low maintenance, easily replaceable and effective passive damping devices, SPPD and ADD, to be implemented with benchmark building to establish their effectiveness in seismic response control.

Table 3. Details of seismic excitations with predominant frequencies

Seismic Excitation	Peak Acceleration (g)	Peak Velocity (cm/sec)	Peak Displacement (cm)	Predominant Frequency (Hz)
El Centro	0.32	31.50	14.13	1.95, 2.68, 6.71
Hachinohe	0.23	25.63	7.42	1.04, 1.68, 2.15
Kobe	0.34	27.67	9.69	2.93, 4.76
Northridge	0.57	51.820	9.03	6.10

4. Hysteresis behavior of SPPD and ADD

Passive damping devices, SPPD and ADD, when tested under varying forcing frequencies and amplitude sinusoidal excitation, demonstrated a tilted elliptical hysteresis loop from its mean position, indicating energy dissipation capabilities due to particle-particle and particle-wall interaction. The hysteresis behavior of SPPD and ADD were studied in terms of parameters, frequency, amplitude, displacement, velocity and damper force under sinusoidal input. Peak displacement of the SPPD and ADD were plotted for steady-state conditions. A peak velocity plot was also plotted to understand the effect of the damping characteristic. Overall hysteresis behavior of SPPD and ADD was studied under four categories: (i) effects of frequency dependency, (ii) effect of amplitude dependency, (iii) effect of velocity dependency, and (iv) frequency-dependent damper force.

4.1 Effects of Frequency Dependency

Damper force produced by SPPD and ADD damping devices under three peak displacement amplitudes as indicated by Table 4 were derived for varying frequencies. Figure 4(a) to Figure 4(c) show the damper force vs displacement relationship of SPPD and ADD, respectively. It has been observed that, each damper device has energy dissipation capability as the damper force to displacement relationship yields a hysteresis loop. It is evident that damper force is a function of the forcing frequency of displacement input since damper force increases with an increase in forcing frequency. This is due to the elastic deformation of silicone rubber particles as the piston transfers the force through particle-

particle interaction. An increase in damper force for each device for a given amplitude of displacement function can be verified from Table 4 as well. Further, it can be observed that the hysteresis loop grows with an increase in forcing frequency under a given amplitude of displacement input, indicating an increase in energy dissipation and, thus, improvement in damping.

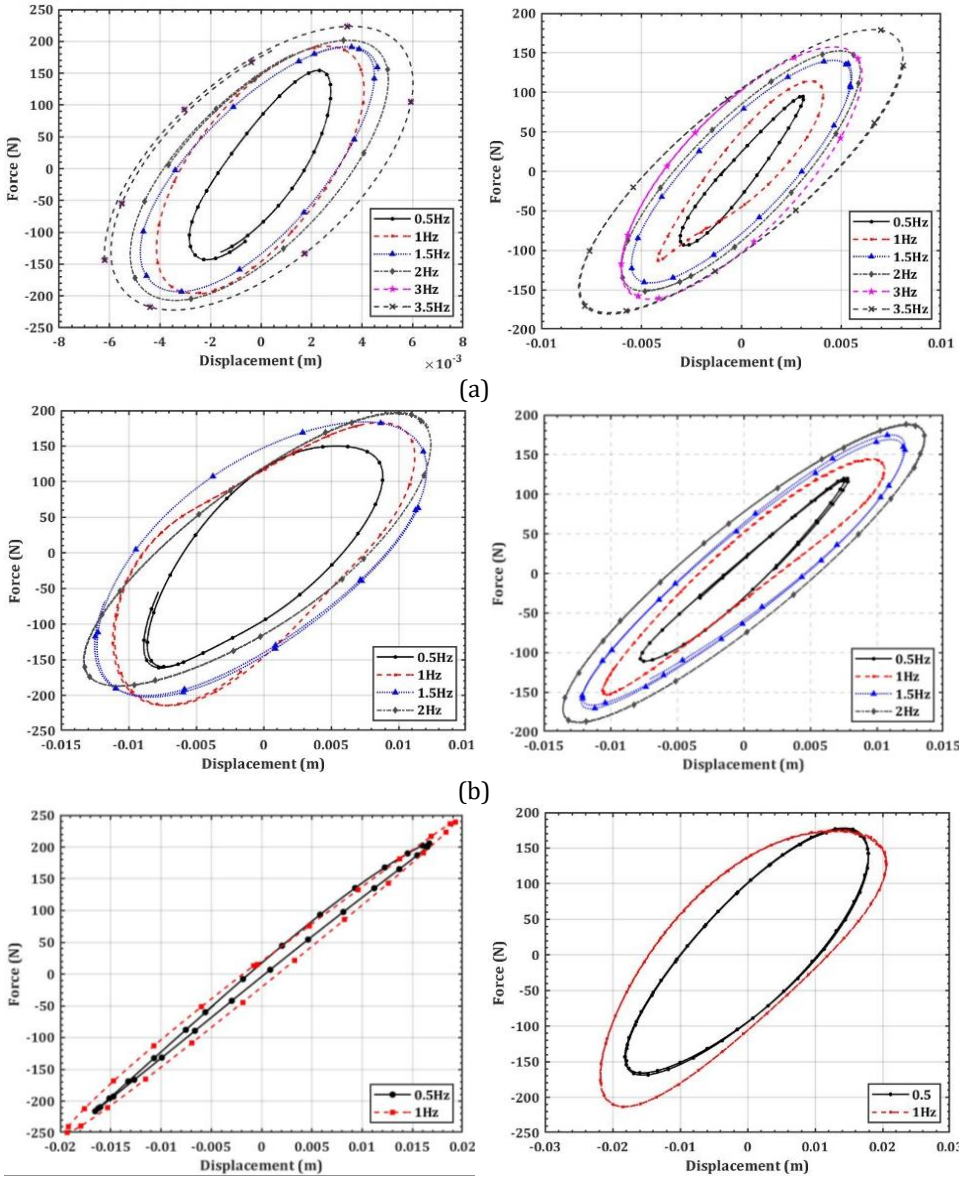

Fig. 4. Hysteresis behavior of SPPD and ADD under variable frequencies of sinusoidal input (a) with displacement amplitude of 5mm (b) with displacement amplitude of 10 mm and (c) with displacement amplitude of 20 mm

Comparing hysteresis loops of SPPD with ADD, it can be concluded that SPPD yields higher damper force and damping coefficient vis-à-vis ADD under each amplitude of displacement input. Hysteresis loops obtained for both SPPD and ADD show a force-displacement relation elliptical, very similar to those of viscous damping devices but with an inclination indicating that passive damping devices are dependent on displacement and velocity of the input motion. This attribute makes them more suitable for seismic response control of building structures as compared to the viscous dampers, which are only velocity dependent. On comparing hysteresis loops with those of reported results [16], it can be realized that level of force and energy dissipation capacities improve a lot.

4.2 Effect of Amplitude Dependency

In order to understand the effect of displacement amplitude on the damping force of SPPD and ADD, damper forces are plotted for various amplitudes under forcing frequencies, 0.5 Hz to 1 Hz. Figure 5(a) and Figure 5(b) show the damper force-displacement relationship for two forcing frequencies, 0.5 Hz and 1 Hz only since high amplitude limits the forcing frequency of the dynamic frame. It is evident that damper force is a function of the amplitude of displacement amplitude input since damper force increases. It can also be realized that SPPD yields a damper higher force as compared to ADD. While increment in the damper force for ADD was quite evident with an increase in displacement amplitude of the sinusoidal input, SPPD yield a similar slight, lower damper force for displacement amplitude of ~10 mm of the input.

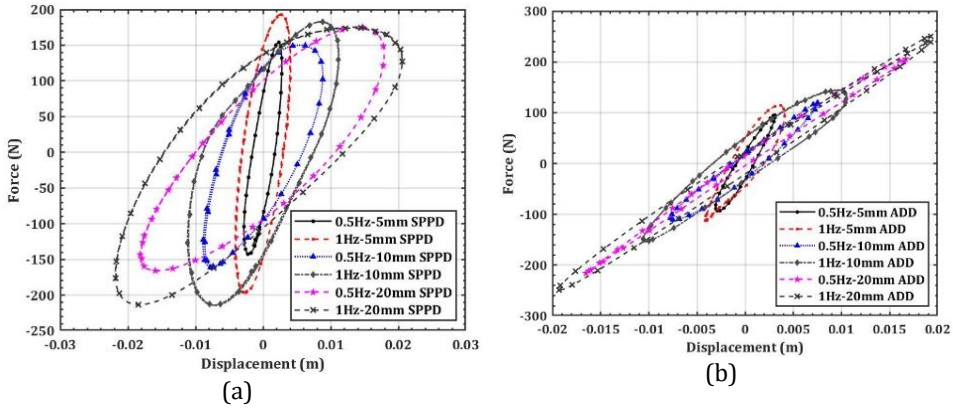

(a) (b)

Fig. 5. Hysteresis behavior of passive damper devices under variable amplitudes of sinusoidal displacement input (a) SPPD with 0.5 Hz and 1 Hz frequencies (b) ADD with 0.5 Hz and 1 Hz frequencies

4.3 Effect of Velocity Dependency Study

The velocity of the SPPD and ADD passive damping devices were plotted against the damping force, as shown in Figure 6(a) to Figure 6(c). It can be realized that stable hysteresis loops observed by the devices indicate that passive damper force is a function of the velocity since it increases with an increase in the velocity. Similar to the displacement damper force relationship, it can be seen that the width of the hysteresis loop increases with higher frequencies, which confirms the energy dissipation capabilities of dampers. It can be observed that with an increase in the forcing frequency of sinusoidal displacement input, the hysteresis loop starts deviating from its vertical portion at low velocity.

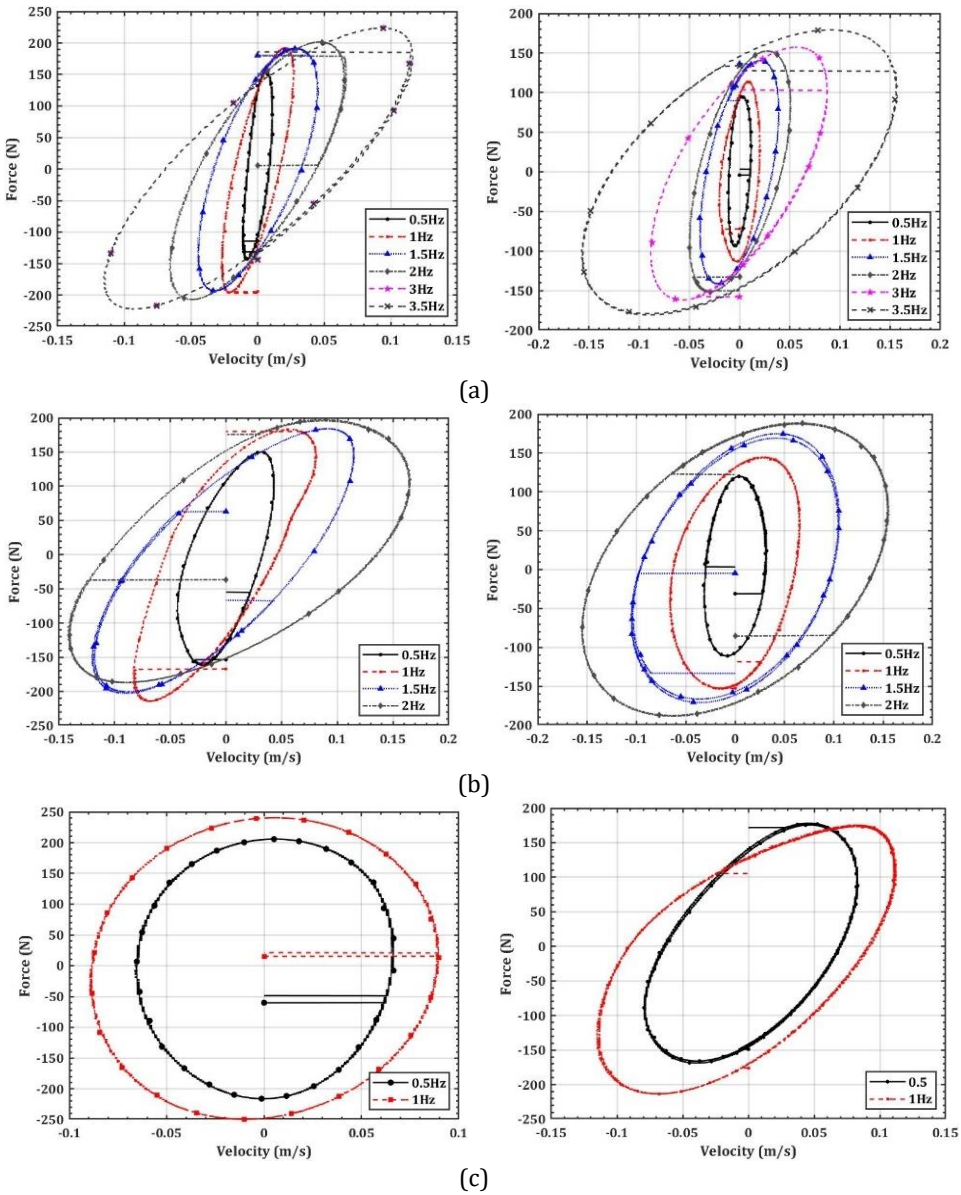

Fig. 6. Hysteresis behavior of SPPD and ADD to input velocity under variable frequencies of sinusoidal input (a) with displacement amplitude of 5mm (b) with displacement amplitude of 10 mm and (c) with displacement amplitude of 20 mm

4.4 Combined Force to Frequency Relationship

In order to study the efficacy of both passive damping devices, SPPD and ADD in terms of their damper force generation capabilities, damper force is plotted against various forcing frequencies of the displacement input. Figure 7 presents a holistic view of damper force to forcing frequencies across all frequencies applied to SPPD and ADD. It is evident that SPPD yields higher damper force as compared to ADD across each forcing frequency and displacement amplitude except for ADD with ~ 20 mm displacement amplitude. It is clearly evident that both damper devices were found effective in generating a reasonable amount

of damper force. However, SPPD outperforms ADD and thus, expected to effectively control seismic parameters of building filled with SPPD.

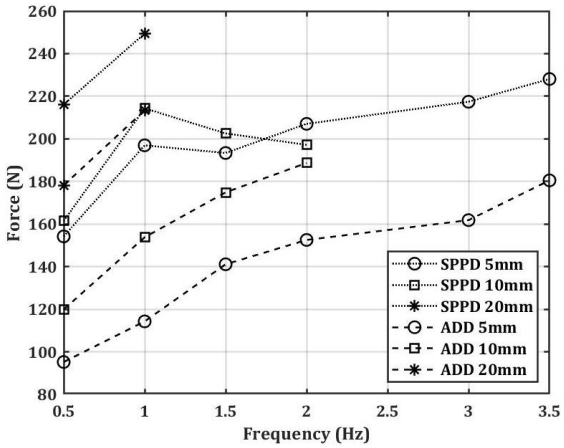

Fig. 7. Damper force produced by SPPD and ADD to various frequencies of sinusoidal displacement input

5. The Kelvin-Voigt Hysteresis Model

It was evident from Figure 4 to Figure 6 that the hysteresis behavior of both SPPD and ADD shows dependency on displacement and displacement rate (velocity) of the sinusoidal input. Therefore, the hysteresis loop obtained from a force-displacement and force-velocity relationship can be represented by an idealized physical model comprising of spring and dashpot elements, as shown in Figure 1(b) subjected to displacement input, producing hysteresis damper force. The said model is popularly known as the Kelvin -Voigt hysteresis model, which gets activated at low displacement and can be fitted well with a linear system and, thus, produces a simplified damper model. The physical model depicted by the physical model as shown in Figure 1(b) has a component of the damper force, the restoring force, proportional to the displacement and another component of the damper force, the damping force, proportional to the velocity and therefore, the damper has the ability to store energy in addition to dissipation energy [10].

Since the Kelvin-Voigt model is a linear combination of two independent variables, 'K' and 'C', the multivariable linear regression method [18] was used to evaluate the variable. A computer program on the MATLAB platform was written to fit experimental data of force with respect to 'K' and 'C'. Coefficient of determination, R^2, was determined for each set of experimental data of force-displacement, and velocity was measured for both SPPD and ADD devices. In order to prove the efficacy of predictive variables 'K' and 'C', the experimental force-displacement relationship was fitted with the force-displacement relationship. A comparison of experimental data of force and predicted plot of force shows very good agreement, which is evident from Figure 8 as well as from the value of R^2, which is tabulated in Table 4. Consistent high values of R^2, i.e. very close to 1 obtained for varying amplitude and forcing frequencies, confirm that the Kelvin-Voigt model with predicted values of variables K and C are well optimized. There is barely any difference visible to force-displacement hysteresis loops for experimentally measured data to that predicted through multivariable linear regression analysis as shown in representative Figure 8(a) for SPPD with 5 mm amplitude and few forcing frequencies and in Figure 8(b) for ADD. It is evident from Table 4 the stiffness values predicted for SPPD vis-a-vis ADD are higher for

a lower amplitude of sinusoidal function and are observed to be decreasing with increasing frequency and amplitude of displacement input.

However, the damping co-efficient, 'C', is found to increase with the amplitude and frequency of sinusoidal displacement inputs for SPPD air to ADD. It can be seen that, the hysteresis loop expands with an increase in amplitudes and forcing frequencies, indicating improvement in energy damping characteristics of the SPPD and ADD devices and thus, both energy dissipation damping devices are expected to be effective in controlling seismic response control of the building in which they are implemented.

Table 4. Damper force under various frequencies and amplitudes of sinusoidal input with stiffness and damping parameters of the Kelvin-Voigt Model

Types of Damper	Forcing Frequency (Hz)	Maximum Force P_{max} (N)	Minimum Force P_{min} (N)	Stiffness K (N/m)	Damping Coefficient C (N.S/m)	Coefficient of Determination R^2
5 mm Amplitude						
SPPD	0.5	154.19	-143.04	40309.41	8000.38	0.9933
ADD		95.21	-93.51	28833.80	2477.95	0.9962
SPPD	1	192.16	-196.96	29955.46	3046.04	0.9966
ADD		114.28	-113.03	21488.60	1977.56	0.9998
SPPD	1.5	191.28	-193.36	30126.35	5443.16	0.9985
ADD		140.47	-141.10	26186.95	2031.12	0.9908
SPPD	2	201.59	-207.05	27013.15	2297.59	0.9985
ADD		152.53	-151.49	20968.58	1724.36	0.9993
SPPD	3	223.56	-221.99	20638.51	1421.67	0.9987
ADD		157.31	-161.83	18031.05	666.13	0.9995
SPPD	3.5	228.10	-225.41	23210.95	1705.25	0.9991
ADD		179.21	-180.50	20144.90	1170.42	0.9990
10 mm Amplitude						
SPPD	0.5	150.07	-161.45	13766.50	2446.54	0.9938
ADD		119.92	-110.91	14705.25	787.13	0.9964
SPPD	1	183.06	-214.33	10068.90	1240.59	0.9984
ADD		144.76	-153.77	13051.67	590.67	0.9992
SPPD	1.5	183.96	-202.56	11285.20	1740.72	0.9900
ADD		174.87	-170.85	13219.88	654.64	0.9951
SPPD	2	197.18	-187.12	11867.58	770.02	0.9965
ADD		188.67	-188.51	12651.02	498.91	0.9998
20 mm Amplitude						
SPPD	0.5	205.67	-216.08	7848.79	1220.05	0.9981
ADD		175.64	-165.92	12821.50	148.61	0.9985
SPPD	1	240.43	-249.44	7076.47	1068.89	0.9896
ADD		175.23	-213.38	12795.54	245.67	0.9993

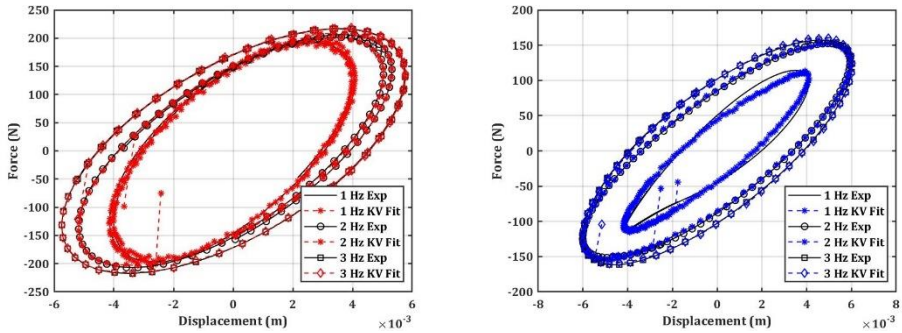

Figure 8: Validation of the Kelvin-Voigt model with experimental data of the force-displacement for sinusoidal displacement amplitude of 5 mm (a) SPPD (b) ADD

6. The Benchmark Building: Problem Formulation

The ASCE committee in 1997 developed a benchmark building problem to innovate various types of dampers for seismic response control and test them against set performance specifications. The present study considers the first generation three-storey benchmark building developed by Spencer et al. [19] as shown in Figure 9. The geometrical properties of the buildings were defined in terms of mass matrix, M and stiffness matrix, K. A Rayleigh damping, which is proportional to the mass and stiffness of the building, is defined as a damping matrix, C. The building is a laboratory based scaled model subjected to seismic excitation at the base. The dynamic equilibrium equation for the said building model can be defined as,

$$\mathrm{M}\,\ddot{\mathrm{x}}(t) + \mathrm{C}\,\dot{\mathrm{x}}(t) + \mathrm{K}\,\mathrm{x}(t) = -\mathrm{M}\,\mathrm{L}\,\ddot{\mathrm{x}}_{\mathrm{g}}(t) \tag{2}$$

where M is a mass matrix, C is a damping matrix, K is the stiffness matrix, L is the influence vector indicating force applied at each floor, x(t), $\dot{x}(t)$ and $\ddot{x}(t)$ are displacement, velocity and acceleration of the mass. The Mass, stiffness and damping matrices are defined by Dyke et al. as,

$$M = \begin{bmatrix} 98.3 & 0 & 0 \\ 0 & 98.3 & 0 \\ 0 & 0 & 98.3 \end{bmatrix} kg; \qquad k = \begin{bmatrix} 12 & -6.84 & 0 \\ -6.84 & 13.7 & -6.84 \\ 0 & -6.84 & 6.84 \end{bmatrix} N/m; \tag{3}$$

$$C = \begin{bmatrix} 175 & -50 & 0 \\ -50 & 100 & -50 \\ 0 & -50 & 50 \end{bmatrix} Ns/m; \qquad L = \begin{bmatrix} 1 \\ 1 \\ 1 \end{bmatrix} N/m; \tag{4}$$

$$K_d = \begin{bmatrix} 19430 & 0 & 0 \\ 0 & 0 & 0 \\ 0 & 0 & 0 \end{bmatrix} N/m; \quad C_d = \begin{bmatrix} 2533 & 0 & 0 \\ 0 & 0 & 0 \\ 0 & 0 & 0 \end{bmatrix} N.s/m; \tag{5}$$

The prototype passive, SPPD and ADD were placed at the ground storey of the benchmark building to control the seismic response of the building. The passive damping devices offered damper force as described by the Kelvin-Voigt model, and thus, the dynamic equilibrium equation stated by Equation (2) will be modified as,

$$\mathrm{M}\,\ddot{\mathrm{x}}(t) + \mathrm{C}\,\dot{\mathrm{x}}(t) + \mathrm{K}\,\mathrm{x}(t) + \mathrm{F_d}\,(t) = -\mathrm{M}\,\mathrm{L}\,\ddot{\mathrm{x}}_{\mathrm{g}}(t) \tag{6}$$

Substituting Equation (2) into Equation (6), the dynamic equilibrium equation becomes,

$$M\,\ddot{x}(t) + (C + C_d)\,\dot{x}(t) + (K + K_d)\,x(t) + F_d(t) = -M\,L\,\ddot{x}_g(t) \quad (7)$$

It is evident from Equation (7) that passive SPPD and ADD improve the damping and stiffness characteristics of the modified benchmark building with the damper. The natural frequencies of the benchmark building model under free vibrion were calculated as, ω_{ni}={5.46, 15.81, 23.64}, rad/sec. where i = 1, 2, 3. The modified natural frequencies of the modal building with damper at ground storey were found to be ω_{ni}={5.52, 15.90, 23.67}, rad/sec. Differential equations, representing modal benchmark buildings with and without passive damping devices; SPPD and ADD, represented through Equation (2) to Equation (7) were subjected to two types of seismic excitation; strong motion and pulse-type. Seismic excitation defined as strong motion are; El Centro excitation (1940, NS component, 3.42 m/s^2 PGA) and Hachinohe excitation (1968, 2.25 m/s^2 PGA), while pulse-type ground motion includes; Kobe excitation (1995, 8.18 m/s^2 PGA) and Northridge excitation (1994, 8.27 m/s^2 PGA).

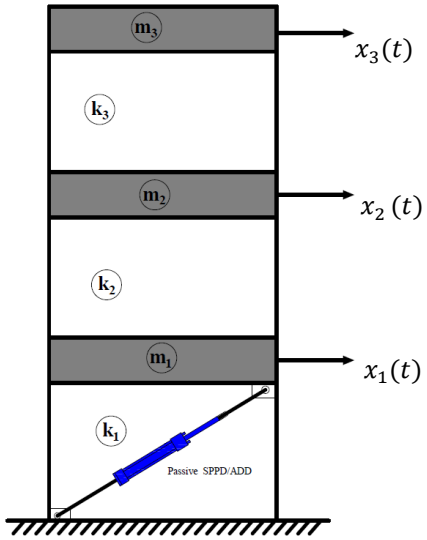

Fig. 9. schematic diagram of first-generation benchmark building filled with passive damping devices; SPPD/ADD

In order to evaluate the efficacy of the prototype passive damping devices, SPPD and ADD, seismic response parameters determined for controlled model building, i.e, model building fitted with SPPD or ADD at the ground storey, were compared with uncontrolled model buildings, i.e., model building without SPPD and ADD fitted to it. The evaluation was carried out through normalized Performance Indices as defined by Ohtori et al. [20], specifically, Peak Interstorey Ratio, J_1, Level Acceleration, J_2, Base Shear, J_3 and Control Force J_{11}. Out of four performance indices considered three indices; J_1, J_2 and J_3 is related to the building response while J_{11} is related to control device. Each of these performance indices are defined as,

$$J_1 = max\left\{\frac{\max_{t,i}\frac{|d_i(t)|}{h_i}}{\delta^{max}}\right\} \qquad J_2 = max\left\{\frac{\max_{t,i}|\ddot{x}_{ai}(t)|}{\ddot{x}_{ai}^{\,max}}\right\} \quad (8)$$

$$J_3=max\left\{\frac{\max_t|\sum_i m_i\ddot{x}_{ai}(t)|}{F_b{}^{max}}\right\} \qquad J_{11}=max\left\{\frac{\max_{t,l}|f_1(t)|}{W}\right\} \tag{9}$$

where $d_i(t)$ is the interstorey drift of the above ground level, h_i is the height of the stories, and δ_{max} is the maximum uncontrolled interstorey drift given by $\frac{|d_i(t)|}{h_i}$, $\ddot{x}_{ai}(t)$ and $\ddot{x}_a{}^{max}$ are the absolute accelerations of i^{th} level for controlled and uncontrolled buildings, respectively. m_i is the seismic mass of the i^{th} level. $F_b{}^{max}$ is maximum uncontrolled base shear, $f_1(t)$ is the force produced by dampers, and W is the seismic weight of the modal building.

7. Results and Discussion

A modal building fitted with passive damping devices, SPPD and ADD, represented by Figure 9, was mathematically modelled as a lumped-mass system and dynamic equilibrium equations defined by Equation (2) to Equation (7) were derived. A Rayleigh damping was assumed for modal building and nonlinear hysteresis behaviour, as characterized under cyclic loading, described in section 3, and was linearized through the linear Kelvin-Voigt model. A detailed computer program on the MATLAB platform was developed to evaluate the seismic response of the benchmark building subjected to strong motion and pulse-type seismic excitation.

Table 5: Validation of uncontrolled structural response with Dyke et al. and controlled structural response of benchmark building under El Centro seismic excitation

Seismic Response Parameters	Storey	Uncontrolled Response		Controlled Response		
		Dyke et al.	Present Study	MR Damper Passive Off Case Dyke et al.	SPPD	ADD
Peak Displacement (cm)	1	0.54	0.55 (-0.02)	0.21 (–60.78)	0.31 (-43.64)	0.41 (-25.46)
	2	0.82	0.87 (6.00)	0.36 (–56.46)	0.52 (-40.23)	0.68 (-21.84)
	3	0.96	1.00 (4.00)	0.46 (–52.70)	0.65 (-38.10)	0.84 (-20.00)
Peak Interstorey Drift (cm)	1	0.54	0.55 (1.85)	0.21 (–60.78)	0.31 (-43.64)	0.41 (-25.46)
	2	0.32	0.34 (6.25)	0.15 (–52.04)	0.22 (-35.29)	0.28 (-17.65)
	3	0.20	0.19 (-5.26)	0.10 (–48.76)	0.13 (-31.58)	0.16 (-15.79)
Peak Acceleration (m/s^2)	1	8.56	8.33 (-2.69)	4.20 (–50.93)	4.32 (-48.13)	5.43 (-34.78)
	2	10.30	10.21 (-0.87)	4.80 (–53.40)	6.31 (-38.19)	8.47 (-17.03)
	3	14.00	13.44 (-4.00)	7.17 (–48.79)	9.03 (-32.78)	11.21 (-16.54)
Damper Force (N)				258.00	277.11	164.73

The numerical solution of Equation (6) was obtained through Newmark-beta numerical integration with the linear acceleration method. The solution was obtained for a time step of 12 seconds, ensuring stability and the accuracy of the numerical solution. Seismic response parameters, peak displacement, peak interstorey drift, peak acceleration and

peak damper force was evaluated for controlled building. The efficacy of passive damping devices, SPPD and ADD considers as passive control devices were evaluated through seismic response performance indices J_1, J_2, J_3 an J_{11}. Uncontrolled model building under strong motion (El Centro, Hachinohe) and pulse type (Kobe, Northridge) seismic excitation was solved first, and seismic response parameter peak displacement, peak intestorey drift, and peak acceleration were determined. The results were validated by comparing them with results represented by Dyke et al. [17] for El Centro seismic excitation. Table 5 summarize seismic response parameters of uncontrolled model building by Dyke et al. and simulation results from the present study with percentage difference provided in the parenthesis. It is evident that results from the present study show close agreement with results for El Centro excitation of Dyke et al. and thus validate numerical simulation carried out through a computer program.

Seismic response parameters of controlled benchmark buildings fitted with SPPD and ADD obtained under seismic excitation are represented in Table 6 with percentage difference in the parenthesis w.r.to uncontrolled response. It is evident that passive damping device, SPPD and ADD, both effectively reduces seismic response parameters. It can be seen that a controlled building with SPPD yields a substantial reduction in each seismic parameter, while it is moderate for ADD-fitted model building. Peak displacement of the roof floor is found to be reduced by 38.10% and 20% controlled building with SPPD and ADD, respectively. Similarly, peak acceleration of the roof storey yields a reduction of 32.88% and 16.54%, respectively. Peak interstorey drift at the first storey shows a reduction of 43.64% and 25.75%, respectively. It can be proved that a double side silicone rubber filled piston-based cylinder, SPPD, device yields better seismic response performance vis-à-vis air filled piston-based cylinder, ADD. This is attributed to elastic deformability and low-hardness silicone rubber. SPPD device can produce damper force of the order 277.11 N which is 68.22% higher as compared to ADD.

Figure 10(a) to Figure 10(d) show the peak displacement response of uncontrolled and controlled buildings for each storey under all seismic excitations considered in the study. It can be observed that the SPPD device yields a substantial reduction in peak displacement at every storey for each seismic excitation. While displacement response shows substantial (~36%-~59%) reduction for El Centro, Hachinohe and Kobe seismic excitations, it is moderate (~13% to 20%) for Northridge seismic excitations since it is of relatively high PGA and consists of a shallow band of earthquake frequencies. It can further be realized that the SPPD device outperformed ADD in terms of peak displacement seismic response performance. Maximum reduction in peak displacement response (~58%) was obtained by a controlled building filled with SPPD and ADD under strong motion type Hachinohe seismic excitation.

Peak interstorey drift for the uncontrolled and controlled model building was determined under each seismic excitation and is plotted through Figure 11(a) to Figure 11(d). It is evident that peak interstorey drift at the first floor shows a substantial reduction under each seismic excitation since SPPD and ADD were provided on the ground floor only. It is apparent that the reduction in peak interstorey drift in upper stories lowered as compared to the first storey. Peak intestorey drift of controlled building with SPPD, at first storey, reduced by 43.64% and 59.68% under El Centro and Hachinohe seismic excitations, respectively and by 40.82% and 20.37% under Kobe and Northridge seismic excitation, respectively. Controlled building with ADD yields a reduction in peak interstorey drift by 25.46%, and 40.32% under El Centro and Hachinohe seismic excitation, respectively and by 21.77% and 11.11% under Kobe and Northridge seismic excitations. It can be realized that the trend of reduction in this seismic response parameter for different seismic excitations storey-wise is very similar to these peak displacements for different seismic excitations.

Table 6. Uncontrolled and controlled structural responses of the benchmark building under Hachinohe, Kobe, and Northridge seismic excitations

Seismic Response Parameter	Storey	Controlled Response								
		Hachinohe Excitation			Kobe Excitation			Northridge Excitation		
		Uncontrolled	SPPD	ADD	Uncontrolled	SPPD	ADD	Uncontrolled	SPPD	ADD
Peak Displacement (cm)	1	0.62	0.25 (-59.68)	0.37 (-40.32)	1.47	0.87 (-40.82)	1.15 (-21.77)	0.54	0.43 (-20.37)	0.48 (-11.11)
	2	0.99	0.40 (-59.60)	0.59 (-40.40)	2.25	1.42 (-36.89)	1.76 (-21.78)	0.74	0.59 (-20.27)	0.65 (-12.16)
	3	1.19	0.49 (-58.82)	0.71 (-40.34)	2.72	1.74 (-36.03)	2.09 (-23.16)	0.79	0.68 (-13.92)	0.72 (-8.86)
Peak Interstorey Drift (cm)	1	0.62	0.25 (-59.68)	0.37 (-40.32)	1.47	0.87 (-40.87)	1.15 (-21.77)	0.54	0.43 (-20.37)	0.48 (-11.11)
	2	0.36	0.15 (-58.33)	0.22 (-38.89)	0.83	0.55 (-33.73)	0.65 (-21.69)	0.28	0.24 (-14.29)	0.26 (-7.14)
	3	0.20	0.08 (-60.00)	0.12 (-40.00)	.520	0.31 (-40.39)	0.41 (-21.15)	0.22	0.18 (-18.18)	0.19 (-13.64)
Peak Acceleration (m/s^2)	1	7.83	3.18 (-59.32)	4.70 (-39.96)	27.20	15.14 (-44.32)	21.35 (-21.51)	15.48	12.04 (-22.23)	13.79 (-10.94)
	2	11.58	4.82 (-58.30)	7.11 (-38.51)	30.72	17.02 (-44.57)	22.52 (-26.69)	12.01	10.06 (-16.20)	11.21 (-6.67)
	3	13.91	5.81 (-58.20)	8.40 (-39.61)	35.91	21.79 (-39.34)	28.63 (-20.29)	14.97	12.65 (-15.49)	13.14 (-12.22)
Peak Damper Force (N)		-	213.42	146.79	-	739.87	497.00	-	328.13	182.35

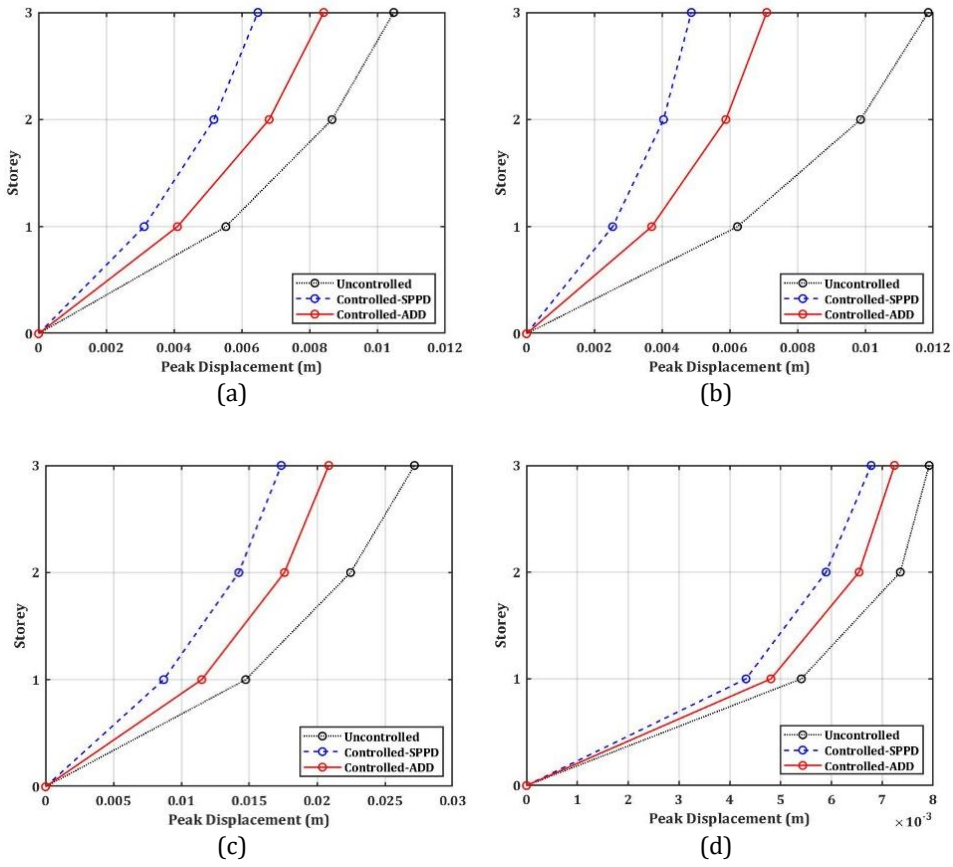

Fig. 10. Peak displacement structural response of uncontrolled and controlled benchmark buildings with SPPD and ADD under seismic excitation (a) El Centro (b) Hachinohe (c) Kobe (d) Northridge

The peak acceleration response of controlled buildings with SPPD and ADD follows similar results in terms of storey-wise reduction as that of peak displacement and peak interstorey drift response parameter. Figure 12(a) to Figure 12(d) demonstrate the storey-wise peak acceleration response of uncontrolled and controlled modelled buildings with passive damping devices. The controlled building attached with SPPD yields a reduction in peak acceleration at each storey under both strong motion and pulse-type seismic excitations. Peak acceleration at the roof storey of the controlled building yields a reduction of 48.13% and 59.32% for El Centro and Hachinohe seismic excitation, respectively. The same reduces by 44.32% and 22.23% for Kobe and Northridge seismic excitation, respectively. On the other hand, ADD fitted with controlled buildings shows a reduction in peak roof acceleration of 34.78%, 39.78%, 21.51% and 10.94% for El Centro, Hachinohe, Kobe and Northridge seismic excitation, respectively. Seismic response parameters, peak displacement, peak interstorey drift, peak acceleration along with peak damper force of SPPD device and ADD of uncontrolled and controlled buildings are reported in Table 6 for all seismic excitations, except El Centro seismic excitation, which is available in Table 5.

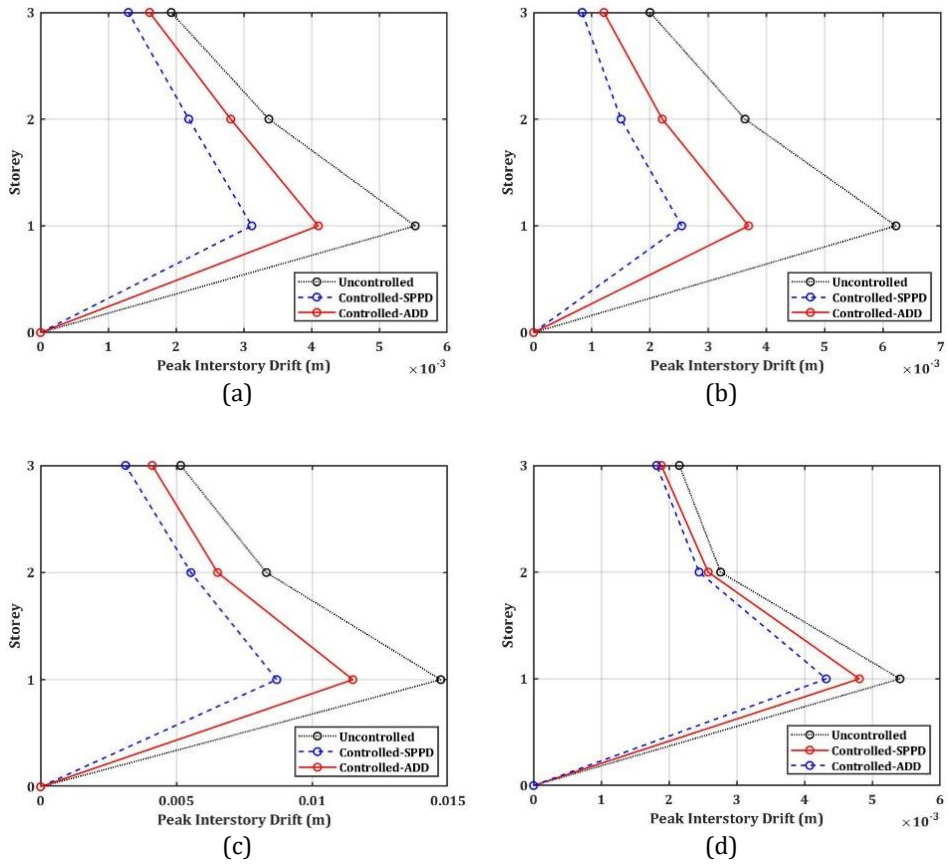

Fig. 11. Peak interstorey structural response of uncontrolled and controlled benchmark buildings with SPPD and ADD under seismic excitation (a) El Centro (b) Hachinohe (c) Kobe (d) Northridge

It is evident from Table 6 that SPPD offers a higher amount of damper force as compared to ADD and, thus, performs better in reducing seismic response parameters. The SPPD warrants a reasonably small amount of damper force under all seismic excitation, except Kobe excitation, where the required damper force is relatively higher. ADD could generate lower damper force vis-à-vis SPPD and, thus, becomes relatively less effective in controlling seismic response parameters. It should be noted that the force generated by SPPD of the present study yields a damper force of the same order or higher when compared with another dual-chamber single-rod-type damper with identical PPR but with higher hardness of silicone rubber [16] which produces force only on the compression side. The efficacy of passive damping devices, SPPD, and ADD, in improving seismic response control of benchmark building has been proved through performance indices defined by Equation (8) and Equation (9) as defined by Ohtori et al. Out of the total performance indices defined [20], only four important PIs most relevant to passive damping devices considered are Peak Interstorey Ratio J_1, Level Acceleration, J_2, Base Shear, J_3 and Control Force, J_{11}. Table 7 summarizes numerical values for PIs J_1, J_2, J_3 and J_{11} under all seismic excitations of the study. It can be observed from the table that both damping devices show good seismic control in terms of parameters represented by PIs as each PIS value < 1.

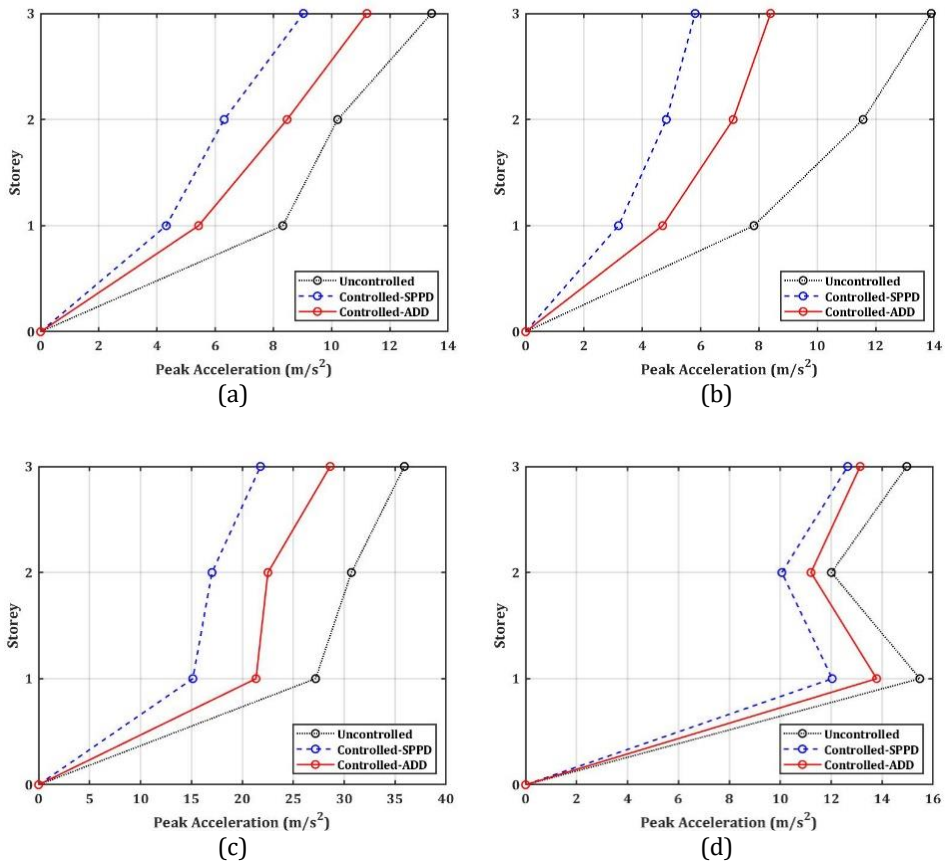

Fig. 12. Peak acceleration structural response of uncontrolled and controlled benchmark buildings with SPPD and ADD under seismic excitation (a) El Centro (b) Hachinohe (c) Kobe (d) Northridge

The lower value of PI- J_1 reveals that the peak interstorey drift of the benchmark building gets better controlled by both SPPD and ADD passive devices. However, the relatively higher value of PI- J_2 indicate that controlling peak acceleration of benchmark buildings under Northridge seismic excitation is a challenge due to the high PGA and low duration of the earthquake. Base shear PI-J_3 depicts a similar understanding as lateral load acting on the benchmark building is higher with respect to weight, thus leading to a higher J_3 value. The lower value of PIs J_1, J_2 and J_3 for SPPD as compared to ADD establishes better efficiency of the former over the latter. The same can be reflected in PI-J_{11}, where values are higher for SPPD vis-à-vis ADD. The relatively lower value of PI-J_{11} for each passive damping device; SPPD and ADD indicate that effective seismic control of benchmark building is achieved with a very low value of the damper fore, which means a handy, low-weight prototype damping device is enough for the seismic control. Peak seismic response parameters, peak displacement, peak interstorey drift, peak acceleration and peak damper force reported in Table 6 and performance indices as shown in Table 7 established well that controlled buildings filled with both passive damping devices, SPPD and ADD perform well vis-à-vis uncontrolled building. A time history response of controlled benchmark building under all seismic excitation considered in the study are plotted in Figure 13 and Figure 14.

Table 7. Seismic response Performance Indices for controlled benchmark building under seismic excitations

Seismic Excitation	Damper Type	Performance Indices				Peak Damper Force (N)
		J_1	J_2	J_3	J_{11}	
El Centro	ADD	0.4692	0.8346	0.7686	0.0569	164.733
	SPPD	0.3568	0.6722	0.5956	0.0958	277.107
Hachinohe	ADD	0.3755	0.6149	0.6071	0.0507	146.793
	SPPD	0.2585	0.4179	0.415	0.0738	213.423
Kobe	ADD	0.4939	0.7971	0.8207	0.1718	497.003
	SPPD	0.3735	0.6066	0.5998	0.2557	739.874
Northridge	ADD	0.5628	0.9333	0.9117	0.0630	182.351
	SPPD	0.5055	0.8451	0.8109	0.1134	328.132

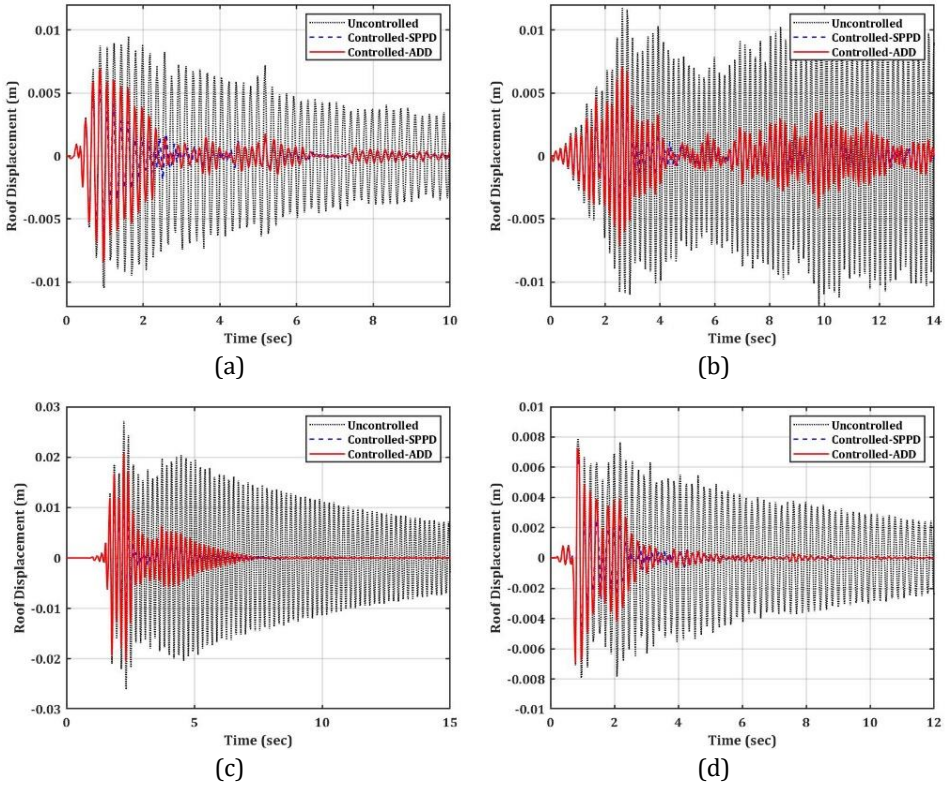

Fig. 13. Roof displacement time history response of uncontrolled and controlled benchmark building under seismic excitation (a) El Centro (b) Hachinohe (c) Kobe (d) Northridge

However, this quantity of controlled benchmark buildings should be plotted with respect to real-time to ensure that passive damping produces the damper force but also remains stable through the presence of seismic excitation. It can be seen that controlled benchmark

buildings with SPPD and ADD yield good displacement control under strong motion and pulse-type seismic excitation throughout the time span as compared to uncontrolled displacement response. The Peak roof displacement of uncontrolled response occurs at 0.96, 9.8, 2.24 and 0.96 sec for El Centro, Hachinohe, Kobe and Northridge seismic excitation, respectively, while the same occurs at 0.96, 2.52, 1.78 and 0.84 sec for controlled response for SPPD. It is evident from Figure 13(a) to Figure 13(d) that the controlled building shows much reduced displacement (almost stopped vibrating) after 7 sec under pulse-type seismic excitation. However, through nicely controlled, displacement of controlled benchmark building sustained under strong motion type seismic excitation, especially, Hachinohe seismic excitation. A similar trend of roof acceleration time history response was achieved for controlled benchmark building under all seismic excitations, as reported in Figure 14(a) to Figure 14(d). Peak roof acceleration of uncontrolled response occurs at 0.98, 9.8, 2.4 and 1.06 sec for El Centro, Hachinohe, Kobe and Northridge seismic excitation, respectively, while the same occurs at 0.96, 2.50, 2.24 and 0.84 sec for controlled response for SPPD. It is evident that both SPPD and ADD passive damping devices are effective in controlling roof acceleration of controlled buildings as compared to uncontrolled buildings under each seismic excitation considered for the study.

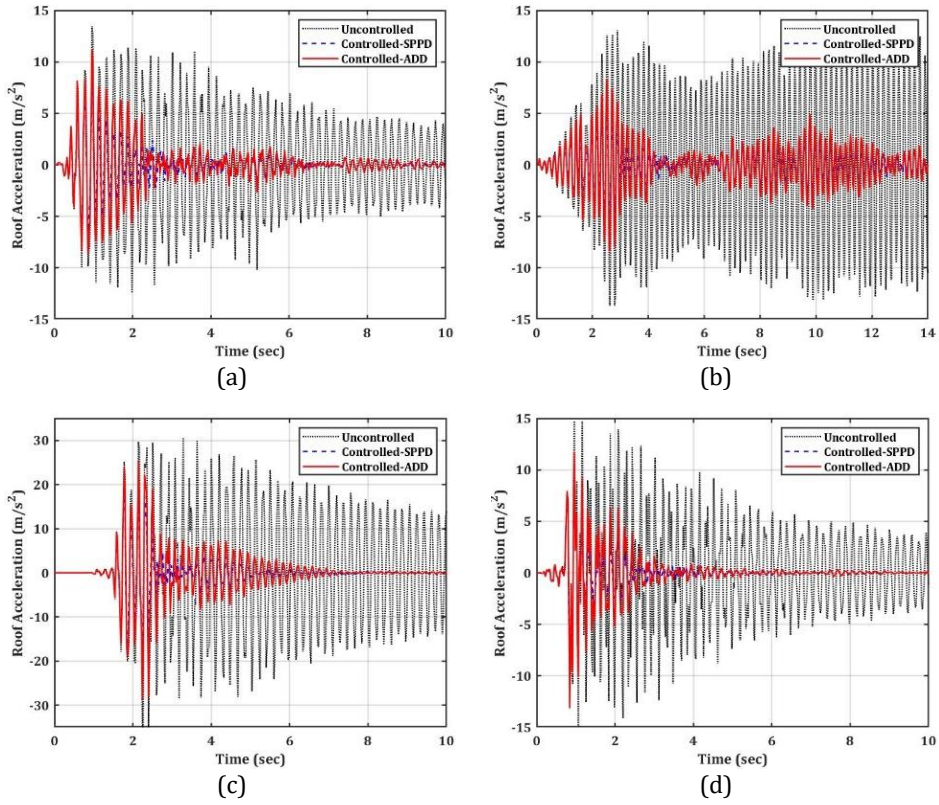

Fig. 14. Roof Acceleration Time History Response of Controlled Model Building to Seismic Excitation (a) El Centro (b) Hachinohe (c) Kobe (d) Northridge

8. Conclusions

Prototype passive damping devices; SPPD, ADD were developed and characterized under varied amplitude and frequency of sinusoidal displacement inputs. Both devices

demonstrate a stable hysteresis loop of elliptical shape, ensuring the presence of viscoelastic properties. Hysterics behaviour was modelled using the Kelvin-Voigt model. SPPD and ADD were fitted at the ground storey of the benchmark building and were subjected to strong ground motion and pulse-type seismic excitations. Seismic response parameters, peak displacement, peak interstorey drift, peak acceleration and peak damper force of controlled benchmark building was evaluated. The efficacy of passive damping devices was established through PIs; J_1, J_2, J_3 and J_{11}. Time history response of roof displacement and roof acceleration were plotted over entire seismic events considered for the study.

Major outcomes derived from the present study are summarized as follows.

- Characterization of SPPD and ADD under sinusoidal input with varied amplitude and frequency exhibits stable hysteresis behaviour, ensuring good damping dissipation characteristics over wide frequencies.
- Parameter identification of the Kelvin-Voigt model by a multivariable linear regression approach yields very good agreement with experimental data of hysteresis curves for SPPD and ADD.
- The SPPD outperforms ADD by yielding a substantial reduction (> 31%) in peak seismic response parameters of the benchmark building when fitted at the ground storey under strong motion and pulse-type seismic excitations. However, under Northridge (pulse-type) seismic excitation the reduction is moderate (>13%).
- The PIs; J_1, J_2, J_3 and J_{11} evaluated for controlled benchmark building establish the efficacy of the SPPD. Though relatively higher than the SPPD, ADD also yields good controlled PIs except J_{11}, which yields a lower value due to the relatively lower damper force produced.
- The Time history response of a controlled benchmark building fitted with SPPD and ADD shows a consistent reduction of roof displacement and roof acceleration over entire seismic events, demonstrating the effectiveness and stability of the damping devices.
- The damper force produced by SPPD and ADD ranges from ~150 N to ~739 N under various seismic excitations, establishing its potential for full-scale implementation.

Seismic response parameters were evaluated for the benchmark building fitted with the SPPD with a particular value of the PPR. Effective seismic response control of the benchmark building with different PPR values for the SPPD using the same or different hardness values of silicone rubber particles may be explored. The proposed passive damping devices, SPPD and ADD may be scaled-up for full-scale implementation.

Acknowledgement

The authors deeply acknowledge the financial assistance received from Nirma University under the minor Research Project for the academic year 2022-2023 and 2023-2024 to conduct the present research work.

References

[1] World Health Organization. Resilient reconstruction: 20 years after Gujarat earthquake [Internet]. 2021 [Accessed January 26, 2021].

[2] Belleri A, Brunesi E, Nascimbene R, Pagani M, Riva P. Seismic performance of precast industrial facilities following major earthquakes in the Italian territory. J Perform Constr Facil. 2015;29(5):1-10. https://doi.org/10.1061/(ASCE)CF.1943-5509.0000617

[3] Nascimbene R. Investigation of seismic damage to existing buildings by using remotely observed images. Eng Fail Anal. 2024;161(April):108282. https://doi.org/10.1016/j.engfailanal.2024.108282
[4] Kaushik HB, Dasgupta K. Assessment of seismic vulnerability of structures in Sikkim, India, based on damage observation during two recent earthquakes. J Perform Constr Facil. 2013;27(6):697-720. https://doi.org/10.1061/(ASCE)CF.1943-5509.0000380
[5] Zhang Y, Fung JF, Johnson KJ, Sattar S. Review of seismic risk mitigation policies in earthquake-prone countries: lessons for earthquake resilience in the United States. J Earthq Eng. 2022;26(12):6208-6235. https://doi.org/10.1080/13632469.2021.1911889
[6] Jain SK. Earthquake safety in India: achievements, challenges and opportunities. Bull Earthq Eng. 2016;14(5):1337-1436. https://doi.org/10.1007/s10518-016-9870-2
[7] Housner GW, Bergman LA, Caughey TK, Chassiakos AG, Claus RO, Masri SF, Skelton RE, Soong TT, Spencer BF, Yao JTP. Structural control: past, present, and future. J Eng Mech. 1997;123:897-971. https://doi.org/10.1061/(ASCE)0733-9399(1997)123:9(897)
[8] Spencer Jr. BF, Nagarajaiah S. State of the art of structural control. J Struct Eng. 2003;129(7):845-856. https://doi.org/10.1061/(ASCE)0733-9445(2003)129:7(845)
[9] Soong TT, Spencer BF. Supplemental energy dissipation: state-of-the-art and state-of-the-practice. Eng Struct. 2002;24(3):243-259. https://doi.org/10.1016/S0141-0296(01)00092-X
[10] Symans MD, Charney FA , Whittaker AS, Constantinou MC, Kircher CA, Johnson MW, McNamara RJ. Energy dissipation systems for seismic applications: current practice and recent developments. J Struct Eng. 2008;134(1):3-21. https://doi.org/10.1061/(ASCE)0733-9445(2008)134:1(3)
[11] Sadek F, Mohraz B, Taylor AW, Chung RM, Kantor M, Prabhakar AA. Passive energy dissipation devices for seismic applications. National Institute of Standards and Technology; 1996. https://doi.org/10.6028/NIST.IR.5923
[12] Lu Z, Wang Z, Zhou Y, Lu X. Nonlinear dissipative devices in structural vibration control: A review. J Sound Vib. 2018;423:18-49. https://doi.org/10.1016/j.jsv.2018.02.052
[13] Lu Z, Wang Z, Masri SF, Lu X. Particle impact dampers: past, present, and future. Struct Control Heal Monit. 2018;25(1):1-25. https://doi.org/10.1002/stc.2058
[14] Bartkowski P, Zalewski R, Chodkiewicz P. Parameter identification of Bouc-Wen model for vacuum packed particles based on genetic algorithm. Arch Civ Mech Eng. 2019;19(2):322-333. https://doi.org/10.1016/j.acme.2018.11.002
[15] Bai XM, Shah B, Keer LM, Wang QJ, Snurr RQ. Particle dynamics simulations of a piston-based particle damper. Powder Technol. 2009;189(1):115-125. https://doi.org/10.1016/j.powtec.2008.06.016
[16] Toyouchi A, Hanai M, Ido Y, Iwamoto Y. Damper force characteristics of a separated dual-chamber single-rod-type damper using an elastomer-particle assemblage. J Sound Vib. 2020;488:1-15. https://doi.org/10.1016/j.jsv.2020.115625
[17] Dyke SJ, Spencer BF, Saint MK, Carison JD. Seismic response reduction using magnetorheological Dampers. Smart Mater Struct. 1996;5(5):565-575. https://doi.org/10.1088/0964-1726/5/5/006
[18] Chapra SC, Canale RP. Numerical Methods for Engineers. McGraw-Hill Education; 2015.
[19] Spencer BF, Dyke SJ, Deoskar HS. Benchmark problems in structural control: Part I - Active Mass Driver system. Earthq Eng Struct Dyn. 1998;27(11):1127-1139. https://doi.org/10.1002/(SICI)1096-9845(1998110)27:11<1127::AID-EQE774>3.0.CO;2-F
[20] Ohtori Y, Christenson RE, Spencer BF, Dyke SJ. Benchmark control problems for seismically excited nonlinear buildings. J Eng Mech. 2004;130(4):366-385. https://doi.org/10.1061/(ASCE)0733-9399(2004)130:4(366)